A Dynamic Decoupling Control Structure for Permanent Magnet Spherical Actuators Based on Active Disturbance Rejection Control

Jingmeng Liu, Huiyang Deng*, Weihai Chen, Jianbin Zhang
School of Automation
Science and Electrical Engineering
Beihang University, Beijing 100191, China
Email: huiyangdeng@foxmail.com

***Abstract*—This paper presents a decoupling control strategy to solve the path following problem for the Permanent Magnet Spherical Actuator (PMSA). The dynamic model can be obtained by the Lagrange-Euler formalism, which is obviously a multi-variable nonlinear system with interactions or cross-couplings. The proposed control structure is based on Active Disturbance Rejection Control (ADRC), one of the main disturbance rejection methods for decoupling control. The dynamic linearization and decoupling is accomplished via a kind of unknown input observer, called Extended State Observer (ESO). It is convinced that ESO can not only estimate the external disturbance, but also plant dynamics. Herein, the linear Active Disturbance Rejection Control (LADRC) is selected for the PMSAs, as the tuning process can be greatly simplified by making all parameters of ESO or the controller a funciton of bandwidth. Simulation results are presented to corroborate the effectiveness of the proposed strategy.**

I. Introduction

Many industrial applications such as manufacturing, underwater vehicles, automobile wheel, or robotic joints require orientation control of the rotating shaft. Conventionally, this type of motion is achieved by connecting a few single-axis actuators in series or in parallel with external mechanism. However, this combined actuation system has intrinsic disadvantages such as bulky structure, large backlash, slow dynamic response, singularity existence in workspace and lack of dexterity. To overcome these drawbacks, the researchers have proposed the concept of spherical actuator, which can realize three degree-of-freedom (3-DOF) motion in one joint.

In the last few decades, various designs of a high performance 3-DOF actuator has been highlighted in a lot of papers. One of the earliest type is the ultrasonic spherical motor, which is based on the reverse piezoelectric[1], [2]. The advantage of this motor is its high resolution, while the shortcomings are small working range, complex fabrication and hysteresis. Recently, the spherical motors based on electromagnetic principles are designed by many researchers. A Spherical Wheel Motor (SWM), an alternative design built on the concept of a Variable Reluctance Spherical Motor (VRSM) developed by Lee decouples the spin from the inclination[3], [4]. Yan has developed a 3-DOF PM spherical actuator, which features the flexible structure[5]. Xia et al. presented a novel halbach array Permanent Magnet Spherical Motor (PMSM). By applying Halbach array to the PMSM, the magnetic field distribution is more sinusoidal, resulting in improving air gap filed distribution and suppressing the torque ripple as well[6], [7]. In this paper, we focus on a Permanent Magnet Spherical Actuator (PMSA) since it has many advantages such as small size, light weight, simple structure, high torque, low cost and so on.

In order to achieve the high performance of a spherical actuator, many control methods have been developed. One typical example is to use the proportional derivative (PD) control law[8], [9]. The PD control has the advantages of simplicity in design and implementation, which leads to acceptable results on many occasions. Nevertheless, it can be inferred from dynamics that the PMSA is a system with complex nonlinearity and strong coupling[4]. In addition, PMSAs are usually subject to parametric uncertainties and external disturbances, so the trajectory tracking performance of the PD control scheme will be seriously affected. To solve these problems, the computed torque method (CTM), which is a model based control scheme, has been widely used in the dynamic control of robotics[10], [11]. In [12] and [13], Artificial Neural Network (ANN) has been applied in the spherical motor, since it has very strong ability of approaching, generalization, and self-adaptation. However, a common back-propagation (BP) algorithm is easy to fall into local minimum, while the advanced one with additional momentum demands extensive training data and a significant computational time.

Considering this matter, an advanced control strategy is required to achieve good performance. Due to the fact that the dynamics of quadrotor helicopter and spherical motor are similar, so the Active Disturbance Rejection Control (ADRC), which has been successfully used in the field of quadrotors[14], [15], is intuitively an excellent choice for PMSAs to improve their trajectory tracking performance. In [16], [17], multi variable system is readily decoupled by estimating and rejecting the effects of both the internal plant

*Corresponding author. e-mail: huiyangdeng@foxmail.com, Tel:+86 010 82315920.

978-1-4673-8644-9/16/$31.00

dynamics and external disturbances.

In this paper, the above ADRC framework is introduced into the dynamic decoupling control of PMSA, where the cross-couplings between control loops as well as external disturbances are treated as disturbance, estimated in real time and canceled in the control law.

II. Dynamic and Torque Model of a PMSA

The mechanical structure of the PMSM is shown in Fig. 1. It consists of a ball-shaped rotor with 8 PM poles in 1 layer and a spherical-shell-like stator with 30 air-core coils in 3 layers. The rotor, supported by a passive spherical joint that contains an encoder and two potentiometers to measure the orientation, can realize tilting and spinning motion within working space. Specifically, as shown in Fig. 2, the upper and lower coils, which are symmetrically respect to the equatorial plane, is responsible for the tilting motion, generated by the attraction or repulsion forces between the coils and permanent magnets, while the the spinning motion is governed by the middle layer coils with a step control approach.

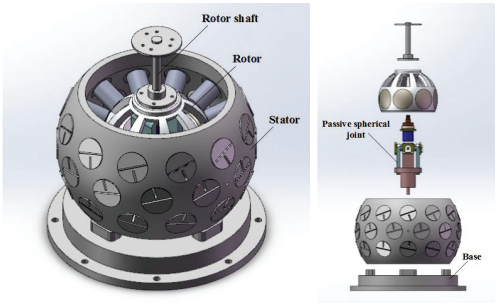

(a) CAD model (b) Explosive view

Fig. 1. The mechanical structure of the PMSA

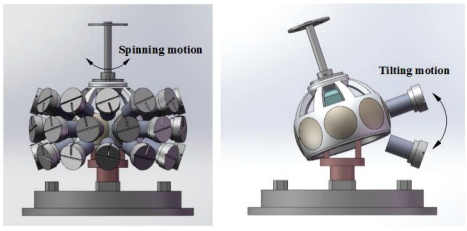

(a) Spinning motion (b) Tilting motion

Fig. 2. The 3-DOF motion of spherical actuator

A. Dynamic Modeling

The rotor orientation is given by a rotation matrix R_{rs} , where $R_{rs} \in SO(3)$ is an orthonormal rotation matrix. The rotation matrix can be obtained through rotations around the axes of the stator at three times. These angles, generally called Euler angles, are bounded as follows: tilting angle α, β, by $(-15° < \alpha, \beta < 15°)$ and spinning angle γ, by $(0° < \gamma < 360°)$.

With these rotations, the following rotation matrix is obtained:

$$R_{\mathrm{rs}} = \begin{bmatrix} c\beta c\gamma & -c\beta s\gamma & s\beta \\ c\gamma s\alpha s\beta + c\alpha s\gamma & c\alpha c\gamma - s\alpha s\beta s\gamma & -c\beta s\alpha \\ -c\gamma s\alpha s\beta + s\alpha s\gamma & c\gamma s\alpha + c\alpha s\beta s\gamma & c\alpha c\beta \end{bmatrix}$$

where and $\mathrm{c}\cdot = \cos(\cdot)$ and $\mathrm{s}\cdot = \sin(\cdot)$.

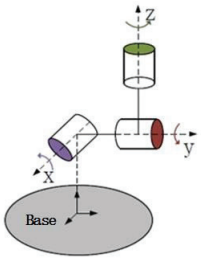

Fig. 3. Coordinate definition

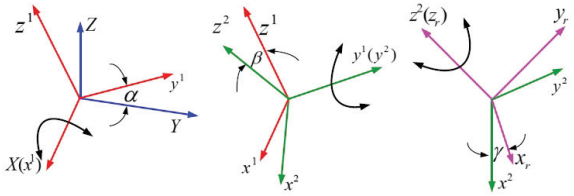

Fig. 4. Euler angles

The dynamic model can be expressed by the Lagrange-Euler formalism based on the kinetic and potential energy concept:

$$M(q)\ddot{q} + C(q,\dot{q})\dot{q} + N(q,\dot{q}) = \tau_c \qquad (1)$$

where

$$\mathrm{q} = [\alpha, \beta, \gamma]^T$$

and

$$M = \begin{bmatrix} m_{11} & m_{12} & m_{13} \\ m_{21} & m_{22} & m_{23} \\ m_{31} & m_{32} & m_{33} \end{bmatrix}$$

where

$$\begin{aligned} m_{11} &= J_1 c^2\beta c^2\gamma + J_2 c^2\beta s^2\gamma + J_3 s^2\beta \\ m_{12} &= (J_1 - J_2) c\beta c\gamma s\gamma \\ m_{13} &= J_3 s\beta \\ m_{21} &= (J_1 - J_2) c\beta c\gamma s\gamma \\ m_{22} &= J_1 s^2\gamma + J_1 c^2\gamma \\ m_{23} &= 0 \\ m_{31} &= J_3 s\beta \\ m_{32} &= 0 \\ m_{33} &= J_3 \end{aligned}$$

and

$$C(q,\dot{q}) = \begin{bmatrix} c_{11} & c_{12} & c_{13} \\ c_{21} & c_{22} & c_{23} \\ c_{31} & c_{32} & c_{33} \end{bmatrix}$$

where

$$\begin{aligned}
c_{11} &= (J_1 c\beta s\beta c^2\gamma - J_2 c\beta s\beta s^2\gamma + J_3 s\beta c\beta)\dot{\beta} \\
&+(-J_1 \mathrm{s}\gamma c\gamma c^2\beta + J_2 c^2\beta s\gamma c\gamma)\dot{\gamma} \\
c_{12} &= (-J_1 c\beta s\beta c^2\gamma - J_2 c\beta s\beta s^2\gamma + J_3 s\beta c\beta)\dot{\alpha} \\
&+((J_1 - J_2)s\beta s\gamma c\gamma)\dot{\beta} + \tfrac{1}{2}(-(J_1 - J_2)c\beta s^2\gamma \\
&+(J_1 - J_2)c\beta c^2\gamma + J_3 s\beta)\dot{\gamma} \\
c_{13} &= -((J_1 - J_2)c\gamma \mathrm{s}\gamma c^2\beta)\dot{\alpha} + \tfrac{1}{2}(-(J_1 - J_2)c\beta s^2\gamma \\
&+(J_1 - J_2)c\beta c^2\gamma + J_3 c\beta)\dot{\beta} \\
c_{21} &= (J_1 c\beta s\beta c^2\gamma + J_2 c\beta s\beta s^2\gamma - J_3 s\beta c\beta)\dot{\alpha} \\
&+\tfrac{1}{2}(-(J_1 - J_2)c\beta s^2\gamma + (J_1 - J_2)c\beta c^2\gamma - J_3 c\beta)\dot{\gamma} \\
c_{22} &= ((J_1 - J_2)c\gamma \mathrm{s}\gamma)\dot{\gamma} \\
c_{23} &= \tfrac{1}{2}(-(J_1 - J_2)c\beta s^2\gamma + (J_1 - J_2)c\beta c^2\gamma - J_3 c\beta)\dot{\alpha} \\
&+((J_1 - J_2)c\gamma s\gamma)\dot{\beta} \\
c_{31} &= ((J_1 - J_2)c\gamma \mathrm{s}\gamma c^2\beta)\dot{\alpha} + \tfrac{1}{2}((J_1 - J_2)c\beta s^2\gamma \\
&-(J_1 - J_2)c\beta c^2\gamma - J_3 c\beta)\dot{\beta} \\
c_{32} &= \tfrac{1}{2}((J_1 - J_2)c\beta s^2\gamma - (J_1 - J_2)c\beta c^2\gamma + J_3 c\beta)\dot{\alpha} \\
&-((J_1 - J_2)c\gamma s\gamma)\dot{\beta} \\
c_{33} &= 0
\end{aligned}$$

and

$$N(q,\dot{q}) = 0 \tag{2}$$

From the above expression, the Lagrange-Euler rotational equations can be written, in general form,as follows:

$$M(\mathrm{q})\ddot{\mathrm{q}} + \mathrm{C}(\mathrm{q},\dot{\mathrm{q}})\dot{\mathrm{q}} = \tau_c \tag{3}$$

Therefore, the mathematical model (used for the controller synthesis) that describes the spherical motor rotational movement obtained from the Lagrange-Euler formalism is given by:

$$\ddot{\mathrm{q}} = -M(\mathrm{q})^{-1}\mathrm{C}(\mathrm{q},\dot{\mathrm{q}})\dot{\mathrm{q}} + M(\mathrm{q})^{-1}\tau_c \tag{4}$$

B. Torque Modeling

The torque modeling of the spherical motor is to establish the relationship between the current input of the stator coils and the torque output. Since the coils are air-core coils, the torque has a linear property with respect to the current. Hence, the torque can be expressed as follows:

$$T = \begin{bmatrix} T_{\mathrm{x}} \\ T_y \\ T_z \end{bmatrix} = GI \tag{5}$$

where the torque matrix G is $G = [G_1 \dots G_j \dots G_N]$ and the current input is $G = [I_1 \dots I_j \dots I_N]^T$. Herein, the value of N is 15, for the coils are divided into 15 groups. G_j describes the torque contribution of current on the jth coil, which is given as

$$G_{\mathrm{j}} = \begin{cases} \sum_{i=1}^{8} (-1)^{i-1} f(\varphi_{ij})(r_i \times s_j / |r_i \times s_j|), r_i \times s_j \neq 0 \\ 0, \qquad\qquad\qquad\qquad\qquad\quad r_i \times s_j = 0 \end{cases} \tag{6}$$

where $f(\varphi_{ij})$ is a torque function between one PM pole and one coil obtained by curve fitting of the computed data using a finite element(FE) method and $\varphi_{ij} = \cos^{-1}(r_i, s_j)$ is the separation angle between the PM pole and the coil.

Therefore, according to Equ. (5), the current inputs at a particular orientation with the desired torque T can be calculated by:

$$I = G^T(GG^T)^{-1}T \tag{7}$$

III. Dynamic Decoupling Control Algorithm Based on ADRC

The nonlinearity and cross-couplings of the spherical motor are unmistakable by observing Equ. (4).

Let

$$\begin{aligned}
\theta_1 &= [\dot{\alpha}, \alpha] \\
\theta_2 &= [\dot{\beta}, \beta] \\
\theta_3 &= [\dot{\gamma}, \gamma] \\
\omega &= [\omega_x, \omega_y, \omega_z] \\
U &= [U_{\tau_x}, U_{\tau_y}, U_{\tau_z}] = \tau_c
\end{aligned} \tag{8}$$

Equ. (4) can be written as follows:

$$\begin{bmatrix} \ddot{\alpha} \\ \ddot{\beta} \\ \ddot{\gamma} \end{bmatrix} = \begin{bmatrix} f_1(\theta_1,\theta_2,\theta_3,w) \\ f_2(\theta_1,\theta_2,\theta_3,w) \\ f_3(\theta_1,\theta_2,\theta_3,w) \end{bmatrix} + M^{-1} \cdot \begin{bmatrix} U_{\tau_\alpha} \\ U_{\tau_\beta} \\ U_{\tau_\gamma} \end{bmatrix} \tag{9}$$

where α, β, γ is the output, ω_{i} is the external disturbances of the ith loop and U is the actual control input.

Herein, define $f = [f_1, f_2, f_3]^T$ as dynamic couplings, since they are independent from control law and define $B(q) = M(q)^{-1}$ as static couplings, since they have an influence in control law.

It is obvious that such two types of couplings should be resolved in different ways.

A. Reformulation of Static Decoupling Control Problem

By introducing the virtual control input:

$$V = M(q)^{-1} \cdot U = \begin{bmatrix} V_{\tau_x} \\ V_{\tau_y} \\ V_{\tau_z} \end{bmatrix} \tag{10}$$

The system Equ. (9) will be transformed as:

$$\begin{bmatrix} \ddot{\alpha} \\ \ddot{\beta} \\ \ddot{\gamma} \end{bmatrix} = \begin{bmatrix} f_1(\theta_1,\theta_2,\theta_3,w) \\ f_2(\theta_1,\theta_2,\theta_3,w) \\ f_3(\theta_1,\theta_2,\theta_3,w) \end{bmatrix} + \begin{bmatrix} V_{\tau_x} \\ V_{\tau_y} \\ V_{\tau_z} \end{bmatrix} \tag{11}$$

The above expression illustrates that three SISO subsystems have been obtained, which describe the relationship between the output α, β, γ and the input $V_{\tau_\alpha}, V_{\tau_\beta}, V_{\tau_\gamma}$, respectively.

In this way, corresponding ADRC controller can be constructed for each subsystem in an attempt to achieve the decoupling control in this square multi variable system.

B. Reformulation of Dynamic Decoupling Control Problem

This MIMO system is too complex to identify how each input affects various output. To address such problem, the dynamic couplings between control loops as well as external disturbances are treated as disturbance, which will be actively estimated and cancelled out in real time. As first shown in [16] for aircraft flight control and then in [18] for high performance turbfan engines, the ADRC has been proved to be a natural solution to disturbance decoupling control (DDC) in the presence of large uncertainties.

The static decoupling control problem is reformulated as disturbance rejection, where the disturbance is defined as the cross channel interference.

Thereby, Equ. (11) can be rewritten as a set of coupled input-output equations with predetermined input-output parings.

$$\begin{cases} \ddot{\alpha} = f_1(\theta_1, \theta_2, \theta_3, w) + V_{\tau_\alpha} \\ \ddot{\beta} = f_2(\theta_1, \theta_2, \theta_3, w) + V_{\tau_\beta} \\ \ddot{\gamma} = f_3(\theta_1, \theta_2, \theta_3, w) + V_{\tau_\gamma} \end{cases} \tag{12}$$

Notably, $\mathrm{f_i}$ represents the combined effect of internal disturbances and external disturbances of the ith loop, containing the interactions among different input-output pairs. The idea of ADRC is to estimate $\mathrm{f_i}$ in real time from a viable change in input-output information rather than by obtaining accurate mathematical description of $\mathrm{f_i}$, which essentially breaks through the limitations of Internal Model Principle (IMP). Hence, Extended State Observer (ESO) is proposed to realize above function.

C. the Design of Extended State Observer (ESO)

The ADRC based ESO is designed for each channel independently. Instead of estimating $\mathrm{f_i}$ off-line, ESO is employed to identify the disturbance in real time.

For the sake of simplicity, Consider one of three channels, the motion of X axis in Equ. (12)

$$\ddot{\alpha} = f_1(\theta_1, \theta_2, \theta_3, w) + V_{\tau_\alpha} \tag{13}$$

Let $x_{1,\alpha} = \alpha, x_{2,\alpha} = \dot{\alpha}$ and $x_{3,\alpha} = f_1$, which is added as an augmented state. Given that $\mathrm{f_1}$ is differentiable, define

$$h_1 = \frac{df_1}{dt} = \dot{f}_1 \tag{14}$$

Then the system Equ. (13) can be expressed in the state space form as:

$$\begin{cases} \dot{x}_{1,\alpha} = x_{2,\alpha} \\ \dot{x}_{2,\alpha} = x_{3,\alpha} + V_{\tau_\alpha} \\ \dot{x}_{3,\alpha} = h_1 \\ y = x_{1,\alpha} \end{cases} \tag{15}$$

where $x_1 = [x_{1,\alpha}, x_{2,\alpha}, x_{3,\alpha}]^T \in R^3$ is the state vector.

Herein, the Linear Extended State Observer (LESO) is designed for such augmented system:

$$\begin{cases} e = \hat{x}_{1,\alpha} - x_{1,\alpha} \\ \dot{\hat{x}}_{1,\alpha} = \hat{x}_{2,\alpha} + l_{1,\alpha} \cdot e \\ \dot{\hat{x}}_{2,\alpha} = \hat{x}_{3,\alpha} + l_{2,\alpha} \cdot e + V_{\tau_\alpha} \\ \dot{\hat{x}}_{3,\alpha} = l_{3,\alpha} \cdot e_1 \end{cases} \tag{16}$$

where $\hat{x}_1 = [\hat{x}_{1,\alpha}, \hat{x}_{2,\alpha}, \hat{x}_{3,\alpha}]^T \in R^3$ is the observed value of state vector x_1 and $l = [l_{1,\alpha}, l_{1,\beta}, l_{1,\gamma}]^T$ is the observer gain parameter vector.

With a well-tuned ESO, the states obtained from the observer will closely track the states of the augmented system. Then ADRC can compensate for f_i in real time by canceling the effect of f_i using $x_{3,\alpha}$, i.e.$\hat{x}_{3,\alpha}$.

D. the Design of Controller

After the state observer properly designed, the controller is constructed as:

$$V_{\tau_\alpha} = \frac{-\hat{x}_{3,\alpha} + V_{\alpha 0}}{b_\alpha} \tag{17}$$

It can be seen from Equ. (11) that b_α is 1. Ignoring the estimation error in $x_{3,\alpha}$, the system is reduced to a unit gain double integration.

$$\ddot{\alpha} = (f_1 - x_{3,\alpha}) + V_{\alpha 0} \approx V_{\alpha 0} \tag{18}$$

which is easily controlled with a PD controller as below:

$$V_{\alpha 0} = k_p(r - x_{1,\alpha}) + k_d x_{2,\alpha} \tag{19}$$

where r is the given trajectory. Note that $-k_d x_{2,\alpha}$, instead of $k_d(\dot{r} - x_{2,\alpha})$, is used to avoid differentiation of the given trajectory and to make the closed-loop transfer function pure second order without a zero.

E. Parameterization of ADRC

Particularly, the above controller Equ. (17) and Equ. (19), combines with the LESO to actively compensate for the disturbances is denoted as Linear Active Disturbance Rejection Control (LADRC). This is a special case of the original ADRC controller, which uses linear gains in place of nonlinear ones in Equ. (16) and Equ. (19).

While the nonlinear gains may be more effective, they also produce extra complexity in the parameter tuning and the proofs of the stability. Thus, the discussion in this paper is limited to the linear case.

In order to simplify the tuning process, bandwidth-parameterizaion is selected for the design of both observer and controller, which refers to assign all eigenvalues at ω_o or ω_c, the making all parameters of the observer and controller become a function of ω_o or ω_c. Here, ω_o is the bandwidth of the observer and ω_c is the bandwidth of the controller. Since it is well known that bandwidth corresponds to the performance of control system. the design specifications can be achieved by adjusting the value of ω_o or ω_c.

Thus, as for ESO, the characteristic equation are chosen as:

$$\lambda_{o,\alpha}(s) = s^3 + l_{1,\alpha}s^2 + l_{2,\alpha}s^2 + l_{3,\alpha} = (s + \omega_{o,\alpha})^3 \tag{20}$$

That is:

$$l_{1,\alpha} = 3\omega_{o,\alpha}, l_{2,\alpha} = 3{\omega_{o,\alpha}}^2, l_{3,\alpha} = {\omega_{o,\alpha}}^3 \tag{21}$$

This makes $\omega_{0,\alpha}$ the only tuning parameter of the X axis. Generally, the larger bandwidth will get an accurate estimation, whereas the thinner bandwidth will produce noise sensitivity. Hence, a compromise between tracking performance and the noise tolerance should be considered.

As for the controller, the characteristic polynomial is obtained in the similar way.

$$\lambda_{c,\alpha}(s) = s^2 + k_d s + k_p = (s + \omega_{c,\alpha})^2 \tag{22}$$

That is:

$$k_p = {\omega_{c,\alpha}}^2, k_v = 2\omega_{c,\alpha} \tag{23}$$

In practice, the bandwidth is tuned based on the requirements of performance, together with the noise sensitivity as well.

IV. Simulation

To evaluate the effectiveness and robustness of the proposed control algorithm, simulations are carried out in this section. The principal inertia moments of the spherical motor are calculated by ADAMS of mechanical system with the solutions as $J_\alpha = 2.219(kg \cdot m^2), J_\beta = 2.176(kg \cdot m^2), J_\gamma = 2.256(kg \cdot m^2)$.

The desired trajectory is:

$$q = \begin{bmatrix} \alpha \\ \beta \\ \gamma \end{bmatrix} = \begin{bmatrix} 15 \cdot \sin(2\pi t) \\ 15 \cdot \cos(2\pi t) \\ 2 \end{bmatrix}, \mathrm{t} \in [0, 3]$$

The internal dynamic are set as follows:

$$\Delta M(q) = 0.2 \cdot M(q), \Delta C(q, \dot{q}) = 0.2 \cdot C(q, \dot{q})$$

where

$$\tilde{J}_\alpha = 1.2J_\alpha, \tilde{J}_\beta = 1.2J_\beta, \tilde{J}_\gamma = 1.2J_\gamma$$

The external disturbance is $\tau_d = 0.02$, which denotes the friction torque.

The design objective is to follow the trajectory in one second with little overshoot, and the physical characteristics of the control problem are: (1)$\tau_c \leq 2N \cdot m$. (2)the sampling rate is 20hz.

Fig. 5 and Fig. 6 show the simulation results of the path following of this reference trajectory. The tunning parameters for ADRC are $\omega_{o,\alpha} = 60, \omega_{c,\alpha} = 5$.

It can be clearly seen from Fig. 6 that the actual trajectory fits the desired trajectory well in less than one second with little overshoot and the interaction of α, β, γ has been eliminated primarily after the control algorithm is applied. Additionally, there is no stead-state tracking error during the motion, illustrating that ADRC is actually a great choice for decoupling control in the presence of the model uncertainty and the load.

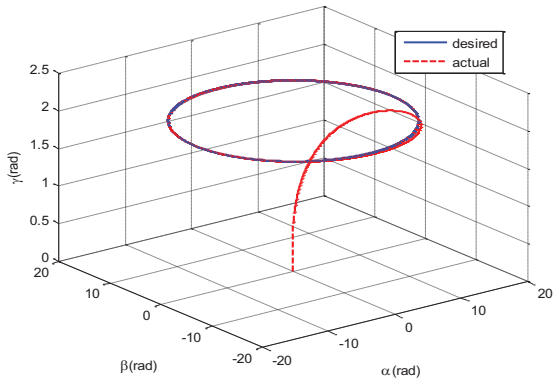

Fig. 5. Trajectory tracking

V. Conclusion

This paper analyzes the trajectory tracking control of the permanent magnet spherical actuators in the presence of internal dynamic and external disturbance. The nonlinear dynamic model with the interactions or cross-couplings among various inputs and outputs has been established based on Lagranges equation, while the torque model has been formulated by FE analysis and a curve fitting method.

In the ADRC frame work, the effect of one input to all other outputs that is not paired with is viewed as disturbance, indicating that ADRC is a natural solution to disturbance decoupling control. Since the PMSA is a multi variable nonlinear system, it is necessary to introduce the concept of virtual control input, in an attempt to eliminate the static couplings among input-output pairs and partition such MIMO system into three SISO subsystem. Nevertheless, the above SISO system is not independent from each other, where the decoupling problem can be reformulated as disturbance rejection. It is obvious that ADRC is a natural solution for this case.

As the core part of the decoupling control system, ESO is chosen as the observer, the new method requires little information of the disturbance. What sets ESO apart from others is that it is convinced to estimate not only the internal dynamics but also the external disturbance.

Notably, the nonlinear structure of ESO with a large number of tuning parameters limits the application in practice. Hence, the linear one is selected instead, as it can simplify the tuning process by bandwidth parameterization. It refers to assigning all observer eigenvalues at bandwidth, of which all parameters of the ESO is a function. What's more, the same parameterization method is employed for the design of the controller.

Finally, the simulation has validated that this control strategy can effectively eliminate the influences of cross-couplings in the PMSAs, together with the external disturbance.

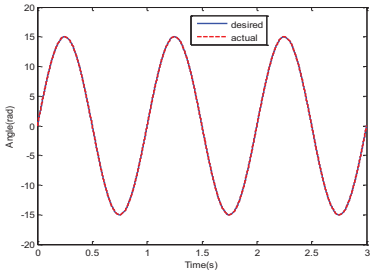

(a) Output response of X

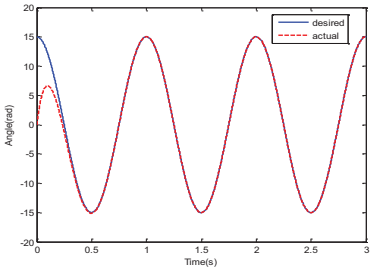

(b) Output response of Y

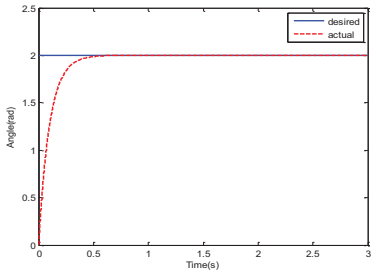

(c) Output response of Z

Fig. 6. Output response for each loop

ACKNOWLEDGMENT

This work is supported by National Nature Science Foundation of China under the research project 51475033, Aeronautical Science Foundation of China under Grant No. 2014ZE51058 and National Natural Science Foundation of China with grant 51475017.

REFERENCES

[1] S. Toyama, S. Sugitani, Z. Guoqiang, Y. Miyatani, K. Nakamura, Multi degree of freedom spherical ultrasonic motor, in: Robotics and Automation, 1995. Proceedings., 1995 IEEE International Conference on, Vol. 3, IEEE, 1995, pp. 2935–2940.

[2] T. Shigeki, Z. Guoqiang, M. Osamu, Development of new generation spherical ultrasonic motor, in: Robotics and Automation, 1996. Proceedings., 1996 IEEE International Conference on, Vol. 3, IEEE, 1996, pp. 2871–2876.

[3] K.-M. Lee, C.-K. Kwan, Design concept development of a spherical stepper for robotic applications, Robotics and Automation, IEEE Transactions on 7 (1) (1991) 175–181.

[4] H. Son, K.-M. Lee, Open-loop controller design and dynamic characteristics of a spherical wheel motor, Industrial Electronics, IEEE Transactions on 57 (10) (2010) 3475–3482.

[5] L. Yan, I. Chen, C. K. Lim, G. Yang, W. Lin, K.-M. Lee, et al., Design and analysis of a permanent magnet spherical actuator, Mechatronics, IEEE/ASME Transactions on 13 (2) (2008) 239–248.

[6] C. Xia, H. Li, T. Shi, 3-d magnetic field and torque analysis of a novel halbach array permanent-magnet spherical motor, Magnetics, IEEE Transactions on 44 (8) (2008) 2016–2020.

[7] C. Xia, P. Song, H. Li, B. Li, T. Shi, Research on torque calculation method of permanent-magnet spherical motor based on the finite-element method, Magnetics, IEEE Transactions on 45 (4) (2009) 2015–2022.

[8] K. Bai, K.-M. Lee, Direct field-feedback control of a ball-joint-like permanent-magnet spherical motor, Mechatronics, IEEE/ASME Transactions on 19 (3) (2014) 975–986.

[9] H. Son, K.-M. Lee, Control system design and input shape for orientation of spherical wheel motor, Control Engineering Practice 24 (2014) 120–128.

[10] K.-M. Lee, R. B. Roth, Z. Zhou, Dynamic modeling and control of a ball-joint-like variable-reluctance spherical motor, Journal of dynamic systems, measurement, and control 118 (1) (1996) 29–40.

[11] W. Wang, J. Wang, G. Jewell, D. Howe, Design and control of a novel spherical permanent magnet actuator with three degrees of freedom, Mechatronics, IEEE/ASME Transactions on 8 (4) (2003) 457–468.

[12] C. Xia, C. Guo, T. Shi, A neural-network-identifier and fuzzy-controller-based algorithm for dynamic decoupling control of permanent-magnet spherical motor, Industrial Electronics, IEEE Transactions on 57 (8) (2010) 2868–2878.

[13] J. Chu, N. Niguchi, K. Hirata, Feedback control of outer rotor spherical actuator using adaptive neuro-fuzzy inference system, in: Sensing Technology (ICST), 2013 Seventh International Conference on, IEEE, 2013, pp. 401–405.

[14] J. WANG, H. MA, W. CAI, H. SHUI, B. NIE, Research on micro quadrotor control based on adrc [j], Journal of Projectiles, Rockets, Missiles and Guidance 3 (2008) 008.

[15] X. Gong, Y. Tian, Y. Bai, C. Zhao, Trajectory tacking control of a quadrotor based on active disturbance rejection control, in: Automation and Logistics (ICAL), 2012 IEEE International Conference on, IEEE, 2012, pp. 254–259.

[16] Y. Huang, K. Xu, J. Han, J. Lam, Flight control design using extended state observer and non-smooth feedback, in: Proceedings of the IEEE Conference on Decision and Control, Vol. 1, IEEE. The Journal's web site is located at http://www. ieeecss. org, 2001, pp. 223–228.

[17] Q. Zheng, Z. Chen, Z. Gao, A practical approach to disturbance decoupling control, Control Engineering Practice 17 (9) (2009) 1016–1025.

[18] R. Miklosovic, Z. Gao, A dynamic decoupling method for controlling high performance turbofan engines, in: Proc. of the 16th IFAC World Congress, 2005, pp. 4–8.